Central European Journal of Energetic Materials
ISSN 1733-7178; e-ISSN 2353-1843

Cent. Eur. J. Energ. Mater. 2022, *19*(1): 91-105; DOI 10.22211/cejem/147766
Article is available in PDF-format, in colour, at:
https://ipo.lukasiewicz.gov.pl/wydawnictwa/cejem-woluminy/vol-19-nr-1/

Research paper

Study of Molecular Perovskite $(H_2dabco)[NH_4(ClO_4)_3]$/ Carbon Nanotubes Energetic Composite

Li-shuang Hu[1)], **Yang Liu**[1,*)], **Dan He**[2)], **Yajun Yang**[3)], **Shida Gong**[1)], **Chunyu Guang**[1)], **Peng Deng**[1,**)], **Shuangqi Hu**[1)]

[1] *School of Environment and Safety Engineering, North University of China, Taiyuan, 030051, China*
[2] *Gan Su Yin Guang Chemical Industry Group CO., LTD, Baiyin, 730900, China*
[3] *Shanxi Jiangyang Xing'an Industrial Explosive Materials CO., LTD, Taiyuan, 030051, China*
**E-mail:* lyang1150@126.com, **nash_deng@163.com

Abstract: An ammonium perchlorate (AP, $NH_4(ClO_4)_3$)-based molecular perovskite energetic material $(H_2dabco)[NH_4(ClO_4)_3]$/carbon nanotubes (DAP/CNTs) composite was prepared and characterized. Molecular perovskite DAP samples were synthesized by a facile one-pot reaction of triethylenediamine, perchloric acid (PCA, $HClO_4$), and AP *via* a molecular assembly strategy. The results showed that the mechanical sensitivity (impact and friction sensitivities: >120 cm and 20%) and electrostatic spark sensitivity (8.90 J) of the DAP/CNTs energetic composite with 10 wt.% CNTs exhibited less sensitivity than that of DAP (impact, friction and electrostatic spark sensitivities: 112.3 cm, 45%, and 5.39 J, respectively), because of the mixing desensitization mechanism of CNTs. Compared with the pure DAP, the DAP/CNTs energetic composite has better performance with respect to thermal stability, exothermic capacity, and excellent continuous combustion properties. The DAP/CNTs energetic composite has potential application in a weapons system.

Keywords: ammonium perchlorate, $(H_2dabco)[NH_4(ClO_4)_3]$, carbon nanotubes, mechanical sensitivity, thermal stability

1 Introduction

As a hot research topic, energetic materials with insensitivity characteristics have received wide attention in the national defense and civil industry. Examples are N-rich compounds, energetic co-crystals, energetic salts, coordination polymers and metal-organic frameworks, *etc*. [1-7]. Consequently, it is important to design and synthesize new high energy density materials with economic, green, and excellent comprehensive performance satisfying practical applications [8, 9].

Chen's group have proposed the idea of molecular assembly strategy [10, 11], based on crystal engineering for the design and fabrication of high-energy explosives with high detonation performance, comparable with even 2,4,6,8,10,12-hexanitrohexaazatetracyclododecane (HNIW) [12], enhanced safety characteristics, and thermal stability. This technique demonstrated the assembly of both organic fuel and oxidizer components into a closely-packed, high-symmetry ternary compound, namely molecular perovskite energetic materials. The outcome resulted in an advanced energetic molecular perovskite with a significant combination of high explosive power as well as high thermal stability, and has attracted more attention from scientific and technological personnel in the area of propellants and explosives. Unlike the complicated synthetic processes for nitrogen-rich energetic organic molecules, such as cyclotrimethylene trinitramine (RDX), cyclotetramethylene tetranitramine (HMX) and HNIW, molecular perovskite energetic materials, which incorporate fuel and oxidizer properties into an organic whole by non-covalent interactions, can be obtained efficiently by a facile, economic, and large-scale one-pot reaction [8, 13-15].

As one of the perchlorate-based molecular perovskites with excellent performance, AP-based molecular perovskite (DAP, $(H_2dabco)[NH_4(ClO_4)_3]$), obtained by the facile one-pot reaction of triethylenediamine, perchloric acid (PCA, $HClO_4$), and AP (molar ratio: 1:2:1), exhibited better detonation performance (theoretical detonation velocity and pressure: 9.588 $km \cdot s^{-1}$ and 49.4 GPa, respectively) [10] than those of the homologous analogues, and is considered to have potential application prospects as the next generation of high-energy-density energetic materials, substituted for nitramine explosives [16]. However, poor mechanical safety characteristics limited their further development and utilization in the military industry and civil industry, due to the intrinsic properties of molecular perovskite, despite the cheap preparation cost. Thus, it is a challenge to regulate and control the safety characteristics of DAP to meet practical requirements.

Carbon nanotubes (CNTs) [17], as an important class of carbon materials, can be used as insensitive additives to reduce the sensitivity of high

sensitivity explosives, due to the outstanding electrical and thermal conductivity of CNTs. According to the hot spot theory of metastable energetic materials [18-20], hot spots can be formed easily from local stress-strain to thermal decomposition under external stimuli, resulting in the ignition of energetic materials. CNTs mixing desensitization technology enhances the interface interaction between the explosives and the CNTs, and efficiently promotes the shifting of hot spots from external stimuli by the good heat conduction of CNTs, making external stimuli insufficient to ignite the energetic materials [21-25]. Therefore, it is significant and promising to modify the safety performances of high sensitivity explosives by CNTs mixing desensitization technology.

In the present paper, the introduction of CNTs to DAP by mixing technology was introduced, and the characteristics of the as-obtained DAP/CNTs energetic composite were investigated. The DAP molecular perovskite samples were synthesized by the facile one-pot reaction of triethylenediamine, PCA, and AP, based on the molecular assembly strategy. Moreover, the sensitivities of raw DAP and DAP/CNTs energetic composite materials were studied by impact, friction, and electrostatic spark sensitivities tests. The results showed that the mechanical and electrostatic spark sensitivities of the DAP/CNTs energetic composite are more insensitive than those of the raw DAP because of the mixing desensitization mechanism. The studies on thermal and combustion of the as-prepared samples suggested that the great exothermic capacity and potential combustion characteristics of the DAP/CNTs energetic composite were increased significantly, however no obvious change was observed in the thermal stability of the energetic composite.

2 Experimental Section

2.1 Materials

AP and PCA (70%) were provided from Shanxi Jiangyang Chem. Eng. Co., Ltd. Triethylenediamine was provided by Shanghai Aladdin Biochemical Technology Co., Ltd. CNTs (95%) were obtained from Nanjing Xianfeng NANO Materials Technology Co., Ltd. Deionized water was obtained from our own laboratory.

2.2 Preparation of DAP and DAP/CNTs composite

DAP was synthesized by the one-pot reaction reported by Chen's group [10]. AP (0.1175 g) and triethylenediamine (0.112 g) were added to water (20 mL). PCA (0.163 mL) was then added to the solution. The mole ratio of AP,

PCA, and triethylenediamine was 1:2:1. Heat was provided until the solid was completely dissolved and the solution was maintained at room temperature. After several days, the as-prepared DAP was obtained by filtration.

The DAP/CNTs energetic composite was fabricated by mechanical mixing. DAP (0.9 g) and CNTs (0.1 g) were added to an agate mortar. The energetic composite was obtained by artificial mixing for 30 min. The small batches were mixed manually and the larger batches were mixed mechanically. The operator must wear a protective suit, safety goggles and protective gloves. A protective baffle was placed between the sample and the operator.

2.3 Characterization

The morphology of nano CNTs and DAP was observed by scanning electron microscopy (SEM, TESCAN Mira3, Brno, Czech Republic) at an accelerating voltage of 5 kV. X-ray diffraction (XRD) patterns were recorded on a Philips X'Pert Pro X-ray diffractometer (PANalytical, Holland) by using Cu-Kα radiation with λ = 0.15418 nm. Fourier transform infrared (FT-IR) spectra were collected on a Nicolet 5700 Fourier spectrometer to test the chemical bonding of the as-obtained samples from 4000 to 400 cm^{-1}, using pressed KBr pellets of the solid samples.

Thermal performance analysis was conducted on a STA449F3 thermogravimetric-differential scanning calorimeter (TG-DSC, Netzsch, Germany) at different heating rates (5, 10, 15, and 20 °C/min). Based on GJB-772A-1997, the impact sensitivity was tested with a WL-1 type impact sensitivity apparatus. The special height (H_{50}) value represents the height from which the 2.0 kg drop-hammer will result in an explosive event in 50% of the trials. Sample masses of 30 mg were tested and 20 drop tests were completed to calculate the H_{50}. The friction sensitivity experiments were measured with a MGY-1 type friction sensitivity instrument. A probability of explosion (in %) was given by 20 tests. Samples of 30 mg each were tested by a 2 kg pendulum hammer, below 90° tilt angle and 3.50 MPa pressure. The electrostatic spark sensitivity experiments were tested by a JGY-50 type electrostatic sensitivity apparatus.

3 Results and Discussions

As fabricated by the facile, green one-pot reaction of AP, PCA, and triethylenediamine at mole ratios of 1:2:1, energetic molecular perovskite DAP samples have a yield of 73.6%. The sizes and morphologies of the samples were characterized by SEM, as shown in Figure 1(a). The results indicated

that micron-sized cubic large particles (side length: ~500 μm) with incomplete morphologies can be obtained from the unstable room-temperature natural crystallization conditions.

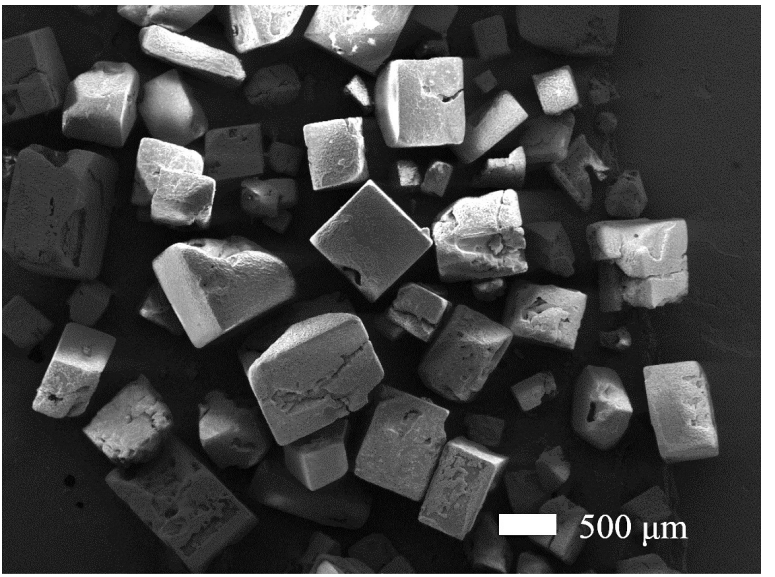

(a)

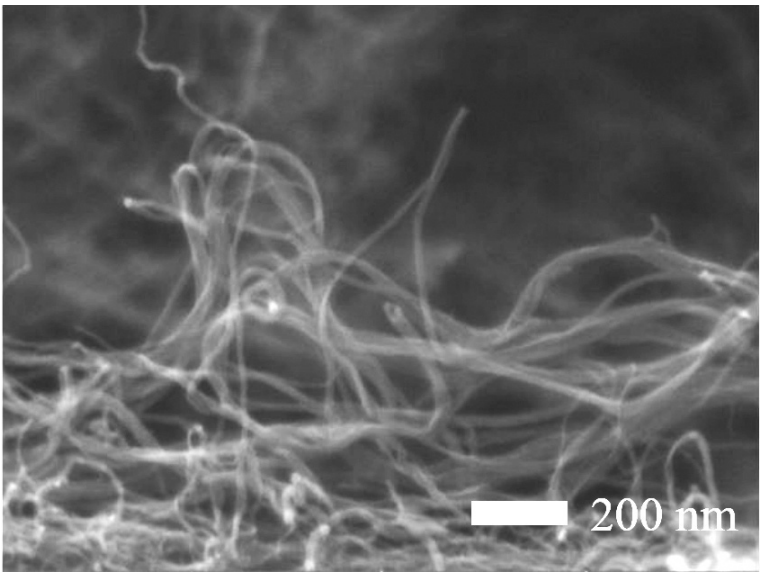

(b)

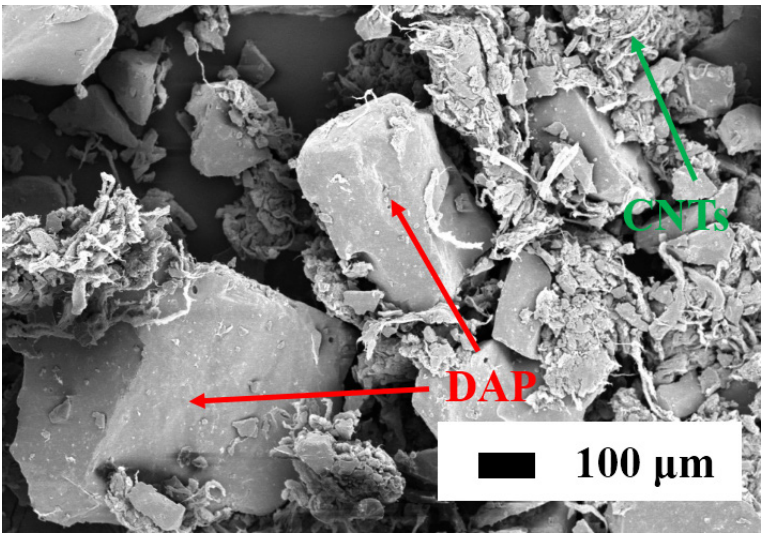

(c)

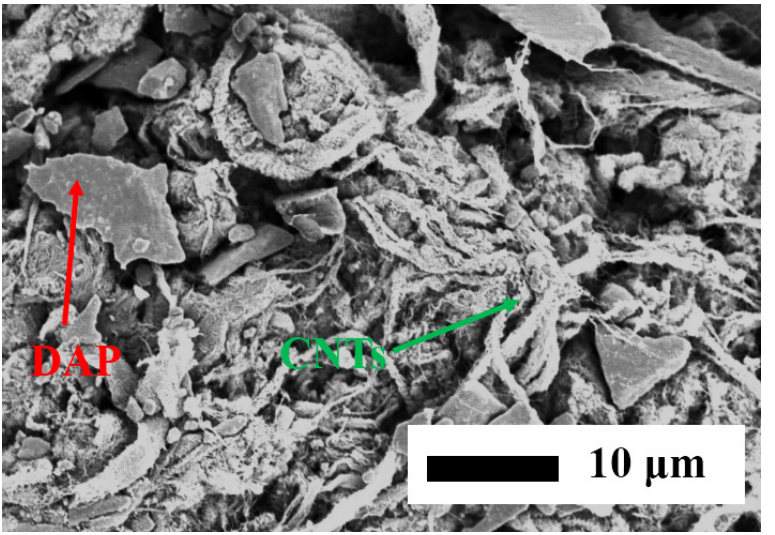

(d)

Figure 1. SEM images of (a) DAP, (b) CNTs, and (c, d) DAP/CNTs energetic composite samples

The XRD patterns of the as-obtained DAP samples and DAP simulation are shown in Figure 2. Sharp diffraction peaks at 21.44, 24.67, 27.7, 36.88, and 39.40°, reflected from (222), (400), (420), (531), and (600), respectively,

suggested high crystallinity of the DAP materials, which are in good agreement with XRD stimulation data (CCDC: 1528108). According to the literature [10], DAP crystals have perovskite-type molecular stacking structures (ABX_3), specifically, in the DAP unit cell, H_2dabco^{2+} acts as the *A* cation, NH_4^+ as the *B* cation, and ClO_4^- as the *X* bridges. A single NH_4^+ is surrounded by twelve O atoms from six ClO_4^- anions by non-covalent interactions, hydrogen bonds. Meanwhile, a ClO_4^- anion can be considered as a bridge with two ambient NH_4^+ ions, forming a three-dimensional anionic framework consisting of cages filled with H_2dabco^{2+} cations. The above characterization results suggested that the energetic molecule perovskite DAP had been synthesized successfully by the molecular assembly strategy.

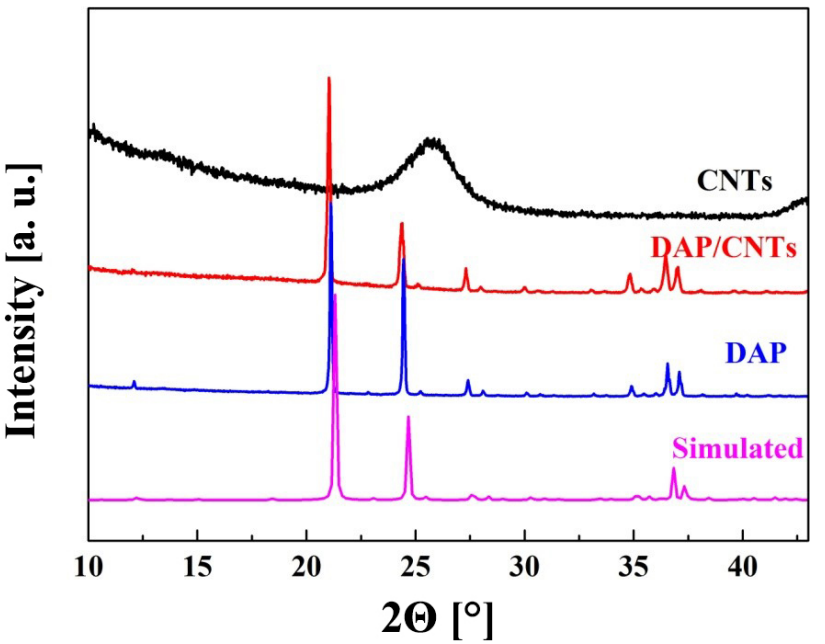

Figure 2. The XRD patterns of CNTs, DAP/CNTs, DAP samples and simulated data

The Raman and FT-IR spectra are shown in Figure 3. The Raman spectrum of DAP samples is shown in Figure 3(a). The characteristic vibrational Raman peak at 3192 cm^{-1} was scattered from NH_4^+, and the peaks at 935, 627, and 437 cm^{-1} from ClO_4^-. For H_2dabco^{2+}, the peaks located at 1469, 1284, and 798 cm^{-1} correspond with the E_{1g} band of N–C deformation, the E_{1g} band of CH_2 twist/C–N rock, and the A_g band of the CH_2 rock, respectively [26-28].

The Raman peaks at 2850-3000 cm^{-1} correspond to C–H stretching vibrations. Additionally, the FT-IR spectrum of DAP is shown in Figure 3(b). The FT-IR spectra of DAP samples exhibited:

– ClO_4^- peaks at 1118 and 627 cm^{-1},
– NH_4^+ peaks at 3451 and 1402 cm^{-1}, and
– H_2dabco^{2+} peaks at 1637 and 1078 cm^{-1}.

The FT-IR and Raman results are consistent.

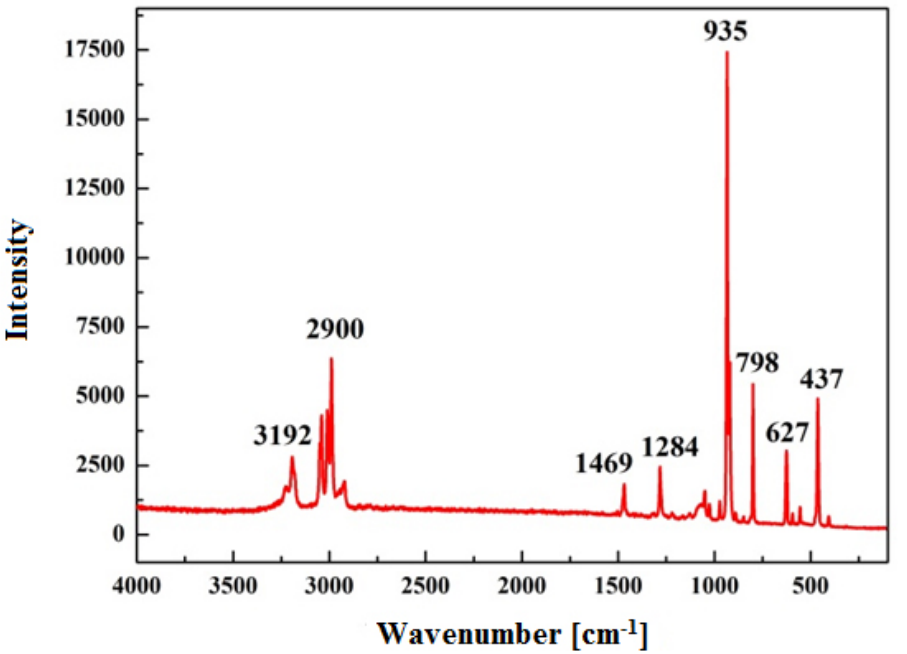

(a)

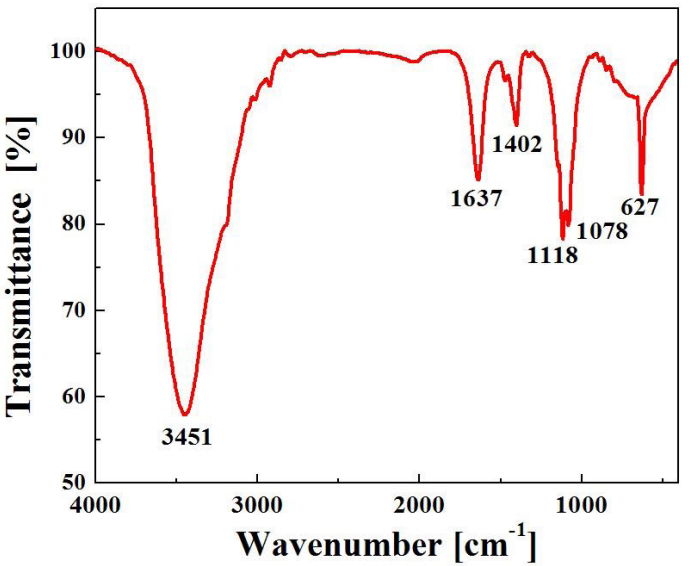

(b)

Figure 3. (a) Raman and (b) FT-IR spectra of DAP

The carbon nanotubes (CNTs) are shown in Figure 1(b). Monodisperse one-dimensional tubulous nanostructures are observed for CNTs. The broadened diffraction peak (002) at 25.7° in Figure 2 demonstrated the presence of CNTs. Furthermore, the DAP/CNTs energetic composite fabricated by mechanical mixing was characterized by XRD in Figure 2. The diffraction peaks at 21.04, 24.38, 27.30, 36.45, and 39.57° reflected from (222), (400), (420), (531), and(600), as in other DAP compositions, respectively. However, the indistinct intensity of the diffraction peak from crystal face (002) of CNTs could not be found because of its low content and the intrinsic contributions of X-ray diffraction. The XRD results suggested that an energetic composite was obtained by simple physical mixing of DAP and CNTs.

The thermal decomposition performance of DAP and DAP/CNTs energetic composite was investigated by TG-DSC measurements as shown in Figure 4 and Table 1. For a pure DAP sample, the endothermic and the exothermic processes can be interpreted by the two peaks located at 274.1 and 385.4 °C, respectively. Heat released from the thermal decomposition process of pure DAP can reach 3421 $J \cdot g^{-1}$. Heat released from the DAP/CNTs energetic composite was less than that from DAP and CNTs, decomposed individually, and the peak temperatures of the energetic composite (endothermic and exothermic peaks: 274.1 and 343.2 °C, respectively) were reduced on addition of CNTs.

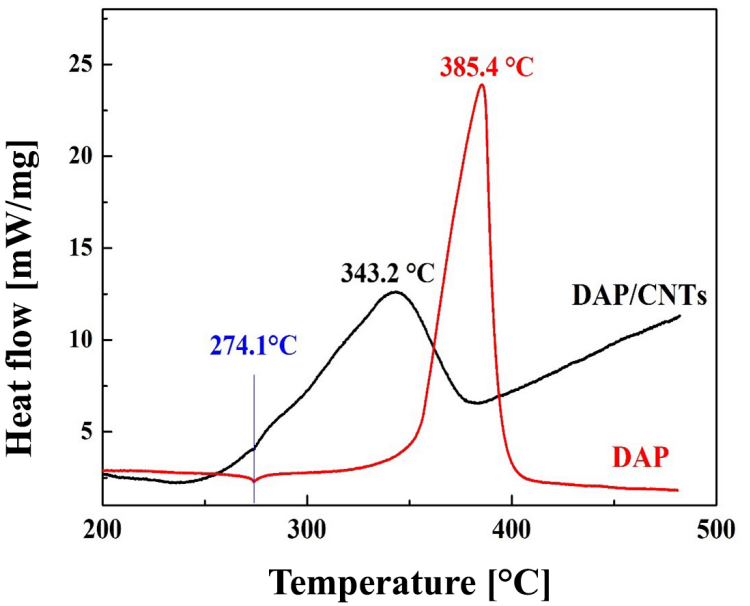

Figure 4. DSC curves of DAP and DAP/CNTs energetic composite

Table 1. Exothermic peak temperature (T_p) and the heat release (ΔH) on thermal decomposition of samples at different heating rates

Sample	T_p [°C]/ΔH [J·g^{-1}], at heating rate [°C·min^{-1}]			
	5	10	15	20
DAP	384.5/3687	385.4/3421	399.7/3084	404.9/3382
DAP/CNTs	318.9/2457	343.2/2601	336.3/2838	342.4/2488

The combustion characteristics of DAP and DAP/CNTs energetic composite are presented in Figure 5. Combustion occurred discontinuously in the combustion process of DAP samples, which exhibited a drastic combustion with fast flame propagation from 1 to 4 ms, and an intermittent one from 5 to 21 ms, resulting from the intrinsic poor self-propagating properties of DAP [29]. For the DAP/CNTs energetic composite, a sustained combustion process was observed from 2 to 28 ms. This showed that the carbon-based fuel, CNTs, in the composite system could participate in a combustion reaction with the oxidizer DAP. By introducing CNTs, more combustion heat can be generated, hence, the produced heat meets the threshold of the surrounding energetic material and thus improves the ability for self-propagation combustion due to the persistent combustion reaction of the CNTs.

Figure 5. The ignition and combustion processes of DAP and DAP/CNTs energetic composite

The impact, friction and electrostatic spark sensitivity tests of pure DAP and DAP/CNTs composite were performed systematically. The results are presented in Table 2. The impact and friction sensitivities were evaluated based on GJB-772A-1997. For impact sensitivity, the DAP/CNTs composite had a special height (H_{50}) above 120 cm, and exhibited greater insensitive than the pure DAP (112.3 cm). For friction sensitivity, the DAP/CNTs composite also exhibited greater insensitivity properties (explosion probability: 20%) than pure DAP (45%). This obviously reduced mechanical sensitivity can be attributed to the CNTs. For mechanical initiation of DAP, hot spots could be formed under external stimuli. Mechanical energy is transformed into thermal energy on the local surfaces of the DAP particles, and DAP can be triggered by thermal energy when local heating exceeds the thermal decomposition threshold of DAP. When CNTs, which have good heat conduction characteristics, are added in the DAP/CNTs system, the thermal conductivity of the system can be greatly improved, which increases the possibility of local heat diffusion. Because of that, the hot spots can shift depending on the heat conduction path of the CNTs. The DAP/CNTs energetic composite has also demonstrated greater insensitivity toward electrostatic spark than DAP alone, resulting from the excellent electroconductibility of CNTs. The above results suggest that the DAP/CNTs energetic composite shows great potential in applications.

Table 2. Impact, friction and electrostatic spark sensitivities of DAP and DAP/CNTs energetic composite

Sensitivity	DAP	DAP/CNTs
Impact sensitivity H_{50} [cm]	112.3	>120
Friction sensitivity [%]	45	20
Electrostatic spark sensitivity [J]	5.39	8.90

4 Conclusions

- In summary, a DAP/CNTs energetic composite was prepared and characterized. DAP was synthesized by the facile one-pot reaction of triethylenediamine, PCA, and AP.
- Mechanical sensitivities (impact and friction sensitivity: >120 cm and 20%) and electrostatic spark sensitivity (8.90 J) of the DAP/CNTs energetic composite showed greater insensitivity than pure DAP (impact, friction and electrostatic spark sensitivity: 112.3 cm, 45%, and 5.39 J, respectively), because of the mixing desensitization mechanism of CNTs.

- The energetic composite has good thermal stability and exothermic capacity, and excellent combustion characteristics, compared with DAP.
- The DAP/CNTs energetic composite has improved application potentials in the field of explosives and propellants over pure DAP.

Acknowledgments

This work was supported by the Fundamental Research Program of Shanxi Province (No. 20210302123030).

References

[1] Xu, Y.; Wang, Q.; Shen, C.; Lin, Q.; Wang, P.; Lu, M. A Series of Energetic Metal Pentazolate Hydrates. *Nature* **2017**, *549*(7670): 78-81.

[2] Zhang, C.; Yang, C.; Hu, B.; Yu, C.; Zheng, Z.; Sun, C. A Symmetric $Co(N_5)_2(H_2O)_4 \cdot 4H_2O$ High-Nitrogen Compound Formed by Cobalt(II) Cation Trapping of a Cyclo-N_5^- Anion. *Angew. Chem. Int. Ed.* **2017**, *129*(16): 4583-4585.

[3] Liu, Y.; Zhang, J.; Wang, K.; Li, J.; Zhang, Q.; Shreeve, J.N.M. Bis (4-Nitraminofurazanyl-3-Azoxy) Azofurazan and Derivatives: 1,2,5-Oxadiazole Structures and High-Performance Energetic Materials. *Angew. Chem. Int. Ed.* **2016**, *128*(38): 11720-11723.

[4] Zhang, J.; Mitchell, L.A.; Parrish, D.A.; Shreeve, J.N.M. Enforced Layer-by-Layer Stacking of Energetic Salts towards High-Performance Insensitive Energetic Materials. *J. Am. Chem. Soc.* **2015**, *137*(33): 10532-10535.

[5] Bolton, O.; Matzger, A.J. Improved Stability and Smart-Material Functionality Realized in an Energetic Cocrystal. *Angew. Chem. Int. Ed*. **2011**, *50*(38): 8960-8963.

[6] Li, S.; Wang, Y.; Qi, C.; Zhao, X.; Zhang, J.; Zhang, S.; Pang, S. 3D Energetic Metal-Organic Frameworks: Synthesis and Properties of High Energy Materials. *Angew. Chem. Int. Ed*. **2013**, *52*(52): 14031-14035.

[7] Cohen, A.; Yang, Y.; Yan, Q.; Shlomovich, A.; Petrutik, N.; Burstein, L.; Pang, S.; Gozin, M. Highly Thermostable and Insensitive Energetic Hybrid Coordination Polymers Based on Graphene Oxide-Cu(II) Complex. *Chem. Mater*. **2016**, *28*(17): 6118-6126.

[8] Zhang, W.; Zhang, J.; Deng, M.; Qi, X.; Nie, F.; Zhang, Q. A Promising High-Energy-Density Material. *Nature Commun.* **2017**, *8*(1): 181-187.

[9] Hu, L.; Liu, Y.; Hu, S.; Wang, Y. 1T/2H Multi-phase MoS_2 Heterostructure: Synthesis, Characterization and Thermal Catalysis Decomposition of Dihydroxylammonium 5,5′-Bistetrazole-1,1′-diolate. *New J. Chem*. **2019**, *43*(26): 10434-10441.

[10] Chen, S.; Yang, Z.; Wang, B.; Shang, Y.; Sun, L.; He, C.; Zhou, H.; Zhang, W.; Chen, X. Molecular Perovskite High-Energetic Materials. *Sci. China Mater*. **2018**, *61*(8): 1123-1128.

[11] Chen, S.; Shang, Y.; He, C.; Sun, L.; Ye, Z.; Zhang, W.; Chen, X. Optimizing the

Oxygen Balance by Changing the A-Site Cations in Molecular Perovskite High-Energetic Materials. *CrystEngComm* **2018**, *20*(46): 7458-7463.

[12] Yu, L.; Ren, H.; Guo, X.; Jiang, X.; Jiao, Q. A Novel ε-HNIW-Based Insensitive High Explosive Incorporated with Reduced Graphene Oxide. *Therm. Anal. Calorim*. **2014**, *117*(3): 1187-1199.

[13] Hu, L.; Du, Z.; Liu, Y.; Gong, S.; Guang, C.; Li, X.; Yang, Z.; Jia, Q.; Liang, K. Green Fabrication of Nanoscale Energetic Molecular Perovskite (H_2dabco)[$Na(ClO_4)_3$] with Reduced Mechanical Sensitivity. *Cent. Eur. J. Energ. Mater*. **2021**, *18*(3): 369-384.

[14] Liu, Y.; Hu. L.; Gong, S.; Guang, C.; Li, L.; Hu, S.; Deng, P. Study of Ammonium Perchlorate-Based Molecular Perovskite (H_2DABCO)[$NH_4(ClO_4)_3$]/Graphene Energetic Composite with Insensitive Performance. *Cent. Eur. J. Energ. Mater*. **2020**, *17*(3): 451-469.

[15] Zhang, J.; Du, Y.; Dong, K.; Su, H.; Zhang, S.; Li, S.; Pang, S. Taming Dinitramide Anions within an Energetic Metal-Organic Framework: A New Strategy for Synthesis and Tunable Properties of High Energy Materials. *Chem. Mater*. **2016**, *28*(5): 1472-1480.

[16] Yan, Q.; Cohen, A.; Petrutik, N.; Shlomovich, A.; Burstein, L.; Pang, S.; Gozin, M. Highly Insensitive and Thermostable Energetic Coordination Nanomaterials Based on Functionalized Graphene Oxides. *J. Mater. Chem. A* **2016**, *4*(25): 9941-9948.

[17] Yan, Q.; Gozin, M.; Zhao, F.Q.; Cohen, A.; Pang, S. Highly Energetic Compositions Based on Functionalized Carbon Nanomaterials. *Nanoscale* **2016**, *8*(9): 4799-4851.

[18] Hu, L.; Hu, S.; Cao, X.; Li, J. Study on the Initiation Capacities of Conical Ring Booster Pellets. *Cent. Eur. J. Energ. Mater*. **2014**, *11*(3): 335-348.

[19] Hu, L.; Gong, S.; Liu, Y.; Li, L.; Guang, C.; Zhi, X.; Hu, S. Fast Cook-Off Analysis of the PBXN-5 Booster Explosive. *Int. J. Energ. Mater. Ch*. **2020**, *19*(4): 307-318.

[20] Hu, L.; Liang, K.; Liu, Y.; Yang, Y.; Du, Z.; Yang, Z.; Li, X.; Lv, T. The p-t Relationship between Booster Pellet and Main Charge under Shock Wave Initiation. *Int. J. Energ. Mater. Ch*. **2021**, *20*(2): 33-46.

[21] Zhang, C. On the Energy & Safety Contradiction of Energetic Materials and the Strategy for Developing Low-Sensitive High-Energetic Materials. *Chin. J. Energ. Mater*. **2018**, *26*(1): 2-10.

[22] Li, R.; Wang, J.; Shen, J.; Hua, C.; Yang, G. Preparation and Characterization of Insensitive HMX/Graphene Oxide Composites. *Propellants Explos. Pyrotech.* **2013**, *38*(6): 798-804.

[23] Liu, T.; Geng, C.; Zheng, B.; Li, S.; Luo, G. Encapsulation of Cyclotetramethylenetetranitramine (HMX) by Electrostatically Self-Assembled Graphene Oxide for Desensitization. *Propellants Explos. Pyrotech.* **2017**, *42*(9): 1057-1065.

[24] Wang, J.; Chen, S.; Yao, Q.; Jin, S.; Zhao, S.; Yu, Z.; Li, J.; Shu, Q. Preparation, Characterization, Thermal Evaluation and Sensitivities of TKX-50/GO Composite. *Propellants Explos. Pyrotech*. **2017**, *42*(9): 1104-1110.

[25] Li, H.; Ren, H.; Jiao, Q.; Du, S.; Yu, L. Fabrication and Properties of Insensitive

CNT/HMX Energetic Nanocomposites as Ignition Ingredients. *Propellants Explos. Pyrotech*. **2016**, *41*(1): 126-135.

[26] Rao, R.; Sakuntala, T.; Deb, S.K. Order-Disorder Transition in Triethylenediamine: A Raman Scattering Study. *J. Mol. Struct*. **2006**, *789*(1-3): 195-199.

[27] Chakraborty, T.; Khatri, S.S.; Verma, A.L. Temperature-Dependent Raman Study of Ammonium Perchlorate Single Crystals: The Orientational Dynamics of the NH^+_4 Ions and Phase Transitions. *J. Chem. Phys.* **1986**, *84*(12): 7018-7027.

[28] Farhadian, A.H.; Tehrani, M.K.; Keshavarz, M.H.; Darbani, S.M.R. Raman Spectroscopy Combined with Principle Component Analysis to Investigate the Aging of High Energy Materials. *Laser Phys.* **2017**, *27*(7): 075701.

[29] Li, X.; Huang, B.; Li, R.; Zhang, H.; Qin, W.; Qiao, Z.; Liu, Y.; Yang, G. Laser-Ignited Relay-Domino-Like Reactions in Graphene Oxide/CL-20 Films for High-Temperature Pulse Preparation of Bi-Layered Photothermal Membranes. *Small* **2019**, *15*(20): 1900338-1900347.

Received: February 21, 2020
Revised: March 28, 2022
First published online: March 31, 2022